Kidney injury molecule–1 is a phosphatidylserine receptor that confers a phagocytic phenotype on epithelial cells

Takaharu Ichimura, Edwin J.P.v. Asseldonk, Benjamin D. Humphreys, Lakshman Gunaratnam, Jeremy S. Duffield, and Joseph V. Bonventre

Renal Division, Department of Medicine, Brigham and Women's Hospital and Harvard Medical School, Boston, Massachusetts, USA.

Following injury, the clearance of apoptotic and necrotic cells is necessary for mitigation and resolution of inflammation and tissue repair. In addition to macrophages, which are traditionally assigned to this task, neighboring epithelial cells in the affected tissue are postulated to contribute to this process. Kidney injury molecule–1 (KIM-1 or TIM-1) is an immunoglobulin superfamily cell-surface protein not expressed by cells of the myeloid lineage but highly upregulated on the surface of injured kidney epithelial cells. Here we demonstrate that injured kidney epithelial cells assumed attributes of endogenous phagocytes. Confocal images confirm internalization of apoptotic bodies within KIM-1–expressing epithelial cells after injury in rat kidney tubules in vivo. KIM-1 was directly responsible for phagocytosis in cultured primary rat tubule epithelial cells and also porcine and canine epithelial cell lines. KIM-1 was able to specifically recognize apoptotic cell surface-specific epitopes phosphatidylserine, and oxidized lipoproteins, expressed by apoptotic tubular epithelial cells. Thus, KIM-1 is the first nonmyeloid phosphatidylserine receptor identified to our knowledge that transforms epithelial cells into semiprofessional phagocytes.

Introduction

Epithelial structures in different organs perform diverse and complex tasks but display stereotyped responses to injury. The kidney epithelium is particularly susceptible to injury due to the character of its blood supply and its ability to concentrate many toxins (1). Injury is characterized by functional deficiencies in handling of salts and water, inability to excrete metabolic toxins, and an innate inflammatory response (2, 3). The damaged segment of the nephron can be remodeled, leading to complete functional recovery, and as such represents a general model of epithelial remodeling after injury. Removal of apoptotic cells and necrotic debris is essential for repair of the tissue with restoration of function (4). Removal of apoptotic cells in a timely fashion has been identified to be a fundamental component of developmental remodeling, regulation of appropriate immune response, and tissue homeostasis (5). It is critical that this process be rapid and efficient to avoid the occurrence of secondary (postapoptotic) necrosis that leads to membrane disruption and leakage of proinflammatory intracellular contents into the tissue. Furthermore, the phagocytic process itself may lead to production of antiinflammatory cytokines (6). Little is known of the process of clearance of apoptotic cells by epithelial cells or the receptors that may be used by these cells (4, 7, 8). Macrophages, professional phagocytes, are rarely seen in the injured epithelial tubule lumen. The goal of these studies was to determine whether kidney injury molecule–1 (KIM-1) plays a role in the phagocytic process in epithelial kidney tubule. KIM-1, also known as TIM-1 (T cell immunoglobulin mucin domains–1), as it is expressed at low levels by subpopulations of activated T cells, and hepatitis A virus cellular receptor–1 (HAVCR-1), expressed by hepatocytes, is a transmembrane protein with extracellular mucin and immunoglobulin domains. KIM-1 is not detectable in the normal human and rodent kidney but is increased in expression more than any other protein in the injured kidney and is localized predominantly to the apical membrane of the surviving proximal epithelial cells (9). KIM-1 is also expressed by dedifferentiated epithelial cells of renal cell carcinomas in humans (10).

In this study, we identified in vivo that apoptotic and necrotic cells of the injured tubule lumen were phagocytosed by surviving epithelial cells that express Kim-1. Furthermore, Kim-1 itself colocalized to the site of internalization of apoptotic cells. Kim-1 confers on epithelial cells the properties of highly phagocytic cells (or semiprofessional phagocytes) and mediates this by binding specifically to phosphatidylserine (PS) and oxidized lipid epitopes on the apoptotic cell surface.

Results

Kim-1–expressing tubule epithelial cells bind and internalize apoptotic bodies and necrotic debris in injured kidneys. Using specific anti–Kim-1 antibodies (9), we localized Kim-1 directly adjacent to apoptotic cells and necrotic debris in the lumens of rat kidney tubules in vivo. Kim-1 also surrounds phagocytosed apoptotic bodies within tubule cells in rat kidney 24 and 48 hours after the kidney had been subjected to ischemic injury (Figure 1, A and B). Confocal images (Figure 1C) confirm internalization of apoptotic bodies within Kim-1–expressing epithelial cells. There are phagocytic cups on the apical surface of tubular cells that are lined with Kim-1 (Figure 1C). Proximal tubules in the outer medulla of the kidney, where injury after ischemia is maximal, were scored for colocalization of Kim-1 staining and the presence of apoptotic bodies (confirmed by TUNEL staining). While 34.6% ± 11.8% of Kim-1–positive

Nonstandard abbreviations used: CMFDA, 5-chloromethylfluorescein diacetate; KIM-1, kidney injury molecule–1; ox-LDL, oxidized LDL; PC, phosphatidylcholine; PE, phosphatidylethanolamine; PS, phosphatidylserine; SRA, scavenger receptor A; tet-off, tetracycline-dependent.

Conflict of interest: T. Ichimura and J.V. Bonventre are coinventors on Kim-1 patents.

Citation for this article: *J. Clin. Invest.* **118**:1657–1668 (2008). doi:10.1172/JCI34487.

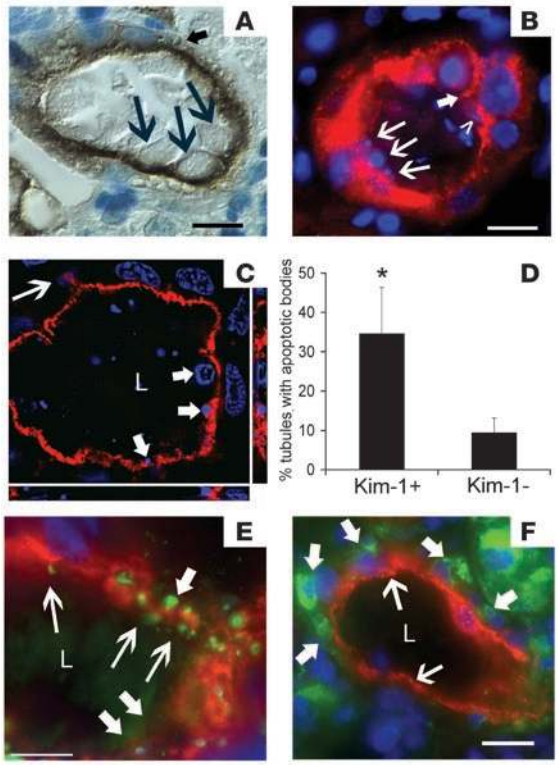

Figure 1
Kim-1–expressing tubule epithelial cells bind and internalize apoptotic bodies and necrotic debris in rat kidneys following ischemic injury. (**A**) By light microscopy, necrotic cellular debris (seen by differential interference contrast [DIC]) binds to apically located Kim-1 (dark brown) of surviving tubule epithelial cells (large arrows). An apoptotic body is seen in 1 Kim-1–positive epithelial cell (small arrow). (**B**) By fluorescence microscopy many DAPI-positive (blue) apoptotic bodies (large arrows) can be seen binding to the surface of Kim-1–positive (red) epithelial cells, and Kim-1–expressing cells have processes (red, small arrow) internalizing an apoptotic body (blue). In addition, apoptotic bodies have been internalized by Kim-1–positive epithelial cells (blue, arrowhead). (**C**) Confocal image of apoptotic cells (blue) localized in phagocytic cups (small arrows) on the Kim-1–positive (red) apical surface of tubular cells. An internalized apoptotic cell is indicated by a large arrow. L denotes the tubule lumen. (**D**) The proportion of Kim-1–positive tubules containing internalized apoptotic bodies was greater than adjacent Kim-1–negative tubules in the post-ischemic kidney. Neither Kim-1 nor apoptotic bodies were identified in the normal kidneys. *P = 0.01 (error bars indicate SD). (**E**) Kim-1–positive epithelial cells (red) binding many TUNEL-positive apoptotic bodies (green, large arrows) and internalizing other small apoptotic bodies (green, small arrow). (**F**) Kim-1–positive epithelial cells (red, large arrows) are surrounded by CD68-positive macrophages (green, small arrows), which do not express Kim-1 and are found only in the interstitium. Scale bar: 10 μm.

tubules contained cell-internalized apoptotic cells, only 9.4% ± 3.7% of Kim-1–negative tubules contained apoptotic cells (Figure 1D). TUNEL-positive nuclei were present in intracellular phagosomes and adherent to the luminal surface of Kim-1–expressing tubules (Figure 1E). Importantly, although macrophages, and to a lesser extent other leukocytes, are recruited to the interstitium of the injured kidney, they are rarely seen within the tubule lumen, where many apoptotic and necrotic cells are seen (Figure 1F) (11). Thus, Kim-1–expressing kidney epithelial cells avidly phagocytose apoptotic and necrotic cells. Note also that Kim-1–expressing cells lack the macrophage marker CD68 and macrophages in the kidney do not express Kim-1 (Figure 1F).

To evaluate the phagocytic properties of Kim-1 in more detail, we cultured primary proximal tubule epithelial cells from mouse and rat kidneys using established methods (12). Primary cultures of rat tubule cells expressed Kim-1 in approximately 25% of cells after 4 days in culture (Figure 2A). Kim-1 was expressed in cytokeratin-expressing cells, confirming their identity as primary tubule epithelial cells (Figure 2B). Monolayers were cocultured for 1 hour at 37°C with 5-chloromethylfluorescein diacetate (CMFDA) fluorescent labeled apoptotic thymocytes, after which noningested apoptotic cells were washed away (Figure 2, A and C). The rat epithelial monolayer was colabeled with antibodies to Kim-1. There was marked binding and phagocytosis of apoptotic cells in Kim-1–expressing but not adjacent Kim-1–negative primary cells. We also observed Kim-1 localized at the phagocytic cup and in the phagosome (Figure 2A). The apoptotic cells associated with Kim-1–positive and Kim-1–negative epithelial cells were determined (Figure 2C). In this assay some apoptotic cells were cell surface bound in addition to others that were phagocytosed. To determine the role of Kim-1 in the phagocytic process directly, coculture with apoptotic cells was carried out in the presence of either monoclonal anti–Kim-1 antibodies with affinity for the ectodomain or isotype control antibodies (Figure 2D). After coincubations and washing, the adherent primary cells were lifted into a single-cell suspension with EDTA and trypsin, and individual suspended epithelial cells were counted by fluorescence microscopy. Kim-1 antibodies markedly inhibited phagocytosis in this assay, indicating that Kim-1 itself played a direct role in phagocytosis (Figure 2D). Further analysis in primary cells could not be undertaken because primary cultured epithelial cells do not survive passaging in vitro and variably exhibit high levels of autofluorescence. In order to study the role of KIM-1 in epithelial cell phagocytosis further, we stably expressed full-length human KIM-1 in porcine LLC-PK1 renal tubular epithelial cell lines (KIM1-PK1 cells) that do not express the native protein (Supplemental Figure 1A; supplemental material available online with this article; doi:10.1172/JCI34487DS1) and also established MDCK II canine kidney epithelial cell lines that could be induced to express KIM-1 by removal of doxycycline (Supplemental Figure 1B). After coculture of KIM1-PK1 cells with apoptotic thymocytes that had been labeled with fluorescent CMFDA, KIM-1 localized initially to the phagocytic cup where apoptotic cells became attached to the epithelial cell surface (Figure 3A, left panel). Later KIM-1 localized to phagosomes that contained apoptotic cells (Figure 3A, right panel). When confocal images were taken of KIM1-PK1 cells labelled with phalloidin to show the actin cytoskeleton, it was clear that apoptotic cells were in phagosomes (Figure 3B). In addition, we generated full-length KIM-1–GFP C terminus–tagged protein and expressed this protein stably in COS-7 cells. Time-lapse images of KIM-1–GFP cells ingesting apoptotic cells showed early recruitment of KIM-1 to the phagocytic cup where initial tethering of the apoptotic cell occurs, followed by further enhancement of the KIM-1 fluorescence in the phagosome after successful engulfment (Supplemental Figure 2 and Supplemental Video 1).

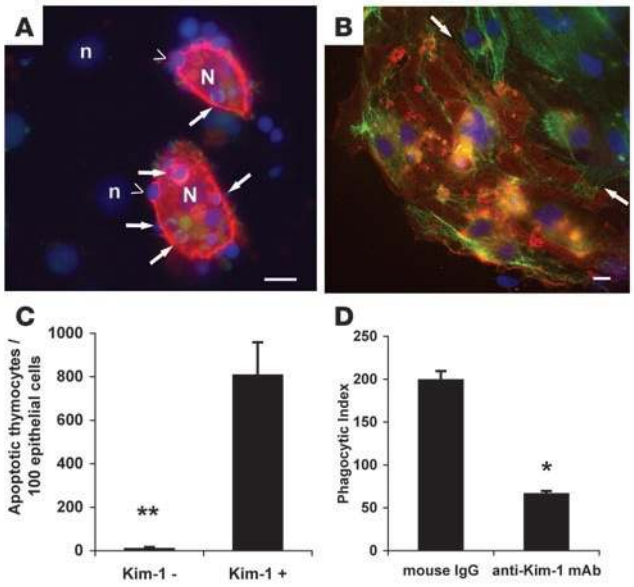

Figure 2
Primary cultured kidney epithelial cells express Kim-1 and phagocytose apoptotic cells by a Kim-1–dependent mechanism. (**A**) Following coculture with apoptotic thymocytes, Kim-1–positive (Kim-1+) (red with blue nuclei [N]) but not Kim-1–negative (Kim-1–) (blue nuclei only [n]) epithelial cells show avid binding (arrowheads) and internalization of fluorescently labeled apoptotic thymocytes (green and blue) (arrows). Note marked ring enhancement of phagosomes with Kim-1, and Kim-1 at the phagocytic cup of bound apoptotic cells. (**B**) Image of primary cultured rat epithelial cells all expressing cytokeratin (green) but showing heterogenous expression of Kim-1 (red). Scale bars: 10 μm. (**C**) The number of apoptotic cells bound or phagocytosed per 100 Kim-1–positive or 100 Kim-1–negative epithelial cells following coculture with labeled apoptotic cells and washing to remove bound cells. Note Kim-1–positive cells show avid phagocytosis. $^{**}P < 0.001$. (**D**) Phagocytic index (number apoptotic cells/100 phagocytes) of Kim-1–positive primary epithelial cell cultures pretreated with monoclonal anti-rat Kim-1 affinity purified antibodies (15 μg/ml) followed by coculture with labeled apoptotic cells. Epithelial cells were lifted from plates and single epithelial cells in suspension scored for phagocytic index. Note that anti–Kim-1 antibodies directed at the extracellular domain block phagocytosis when compared with cells preincubated with isotype control antibodies. $^{*}P < 0.01$.

To quantify phagocytosis using an automated system, KIM-1–expressing KIM1-PK1 cells were cocultured for 1 hour at 37°C with fluorescently labeled apoptotic LLC-PK1 cells or apoptotic thymocytes, after which noningested apoptotic cells were washed away and live cells were lifted into a single-cell suspension with EDTA and trypsin. Bound noninternalized apoptotic cells are removed by this procedure. Compared with LLC-PK1 cells stably transfected with empty vector (pcDNA-PK1), KIM1-PK1 cells more avidly internalized apoptotic cells (Figure 3). When quantitatively assessed by a flow cytometric assay that measures increased fluorescence of epithelial cells in suspension following ingestion of fluorescently labeled apoptotic cells, KIM1-PK1 cells showed approximately 10-fold greater phagocytosis of apoptotic LLC-PK1 cells (14.8% ± 4.2% were positive for apoptotic cells vs. 1.5% ± 0.4% in control cells) and 2-fold greater phagocytosis of apoptotic thymocytes (24.2% ± 1.2% KIM1-PK1 cells vs. 12.0% ± 0.7% pcDNA-PK1 cells) (Figure 4B) (13, 14). Direct fluorescence microscopy of the coincubations that had been analyzed by flow cytometry confirmed marked increases in internalized apoptotic cells; when scored by blinded microscopic counting of random fields (15, 16), 21.5% ± 2.8% of KIM1-PK1 cells internalized apoptotic thymocytes compared with 4.6% ± 1.4% in pcDNA-PK1 cells. Likewise, 30.9% ± 4.8% of KIM1-PK1 cells were observed to phagocytose apoptotic LLC-PK1 cells as compared with 4.4% ± 1.0% of pcDNA-PK1 cells. The phagocytic index was also increased as determined by microscopic scoring (KIM1-PK1 cells, 34.48 ± 2.74 vs. pcDNA-PK1 cells, 4.88 ± 1.13). To be certain that the flow cytometric assays measured phagocytosis and not merely binding, internalization was examined in cocultures incubated at 4°C, a temperature which prevents internalization (17), and at 37°C (Figure 5A). At 4°C, 0.07% ± 0.11% of KIM1-PK1 cells had increased fluorescence, indicative of phagocytosis, whereas at 37°C, 11.34% ± 4.51% of the KIM1-PK1 cells exhibited enhanced fluorescence, indicative of phagocytosis of fluorescent apoptotic cells (Figure 5A). To confirm the specificity of these findings, we used a tetracycline-dependent (tet-off), conditional KIM-1 expression cell system in MDCK canine kidney tubular epithelial cells (Supplemental Figure 1). Phagocytosis of apoptotic

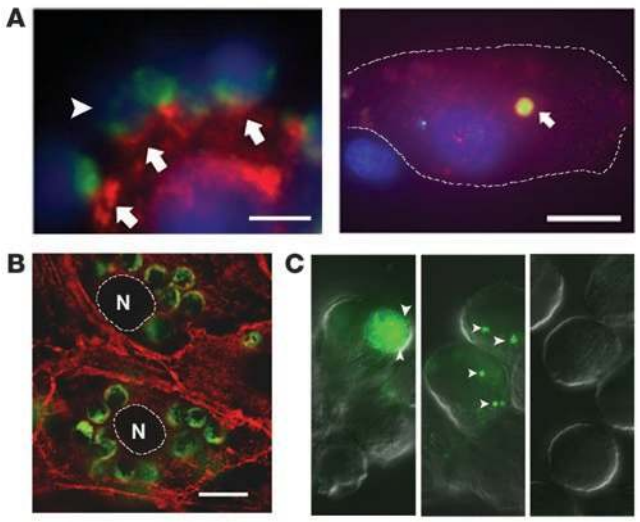

Figure 3
KIM-1–expressing kidney epithelial cell lines avidly bind and phagocytose apoptotic and necrotic material. (**A**) KIM-1 (red) in a KIM1-PK1 cell (left panel) is expressed at high levels (arrows) at the point of binding of multiple apoptotic thymocytes (green and blue) and is part of the initial phagocytic cup (arrowhead). Scale bar: 5 μm. At later time points (right panel), KIM-1 remains associated with the internalized apoptotic cell, resulting in ring enhancement (arrow) of the apoptotic body. The cell border is highlighted by broken lines. Scale bar: 10 μm. (**B**) Multiple apoptotic thymocytes labeled with CMFDA (green) were localized intracellularly in KIM-1–expressing cells after coculture. Internalized apoptotic thymocytes are visualized in the confocal plane of cortical actin filaments (red) in this confocal image confirming internalization. Cell nuclei (N) are highlighted. Scale bar: 10 μm. (**C**) DIC with fluorescence (green) microscopic images of KIM1-PK1 cells confirm ingestion of CMFDA-labeled (green) apoptotic LLC-PK1 cells (left panel) or sonicated LLC-PK1 cell debris (middle panel). pCDNA-PK1 cells in the same experiment showing no phagocytosis of apoptotic cells (right panel). These microscopic studies confirm internalization of fluorescent apoptotic or necrotic cell debris (arrowheads). Original magnification, ×60.

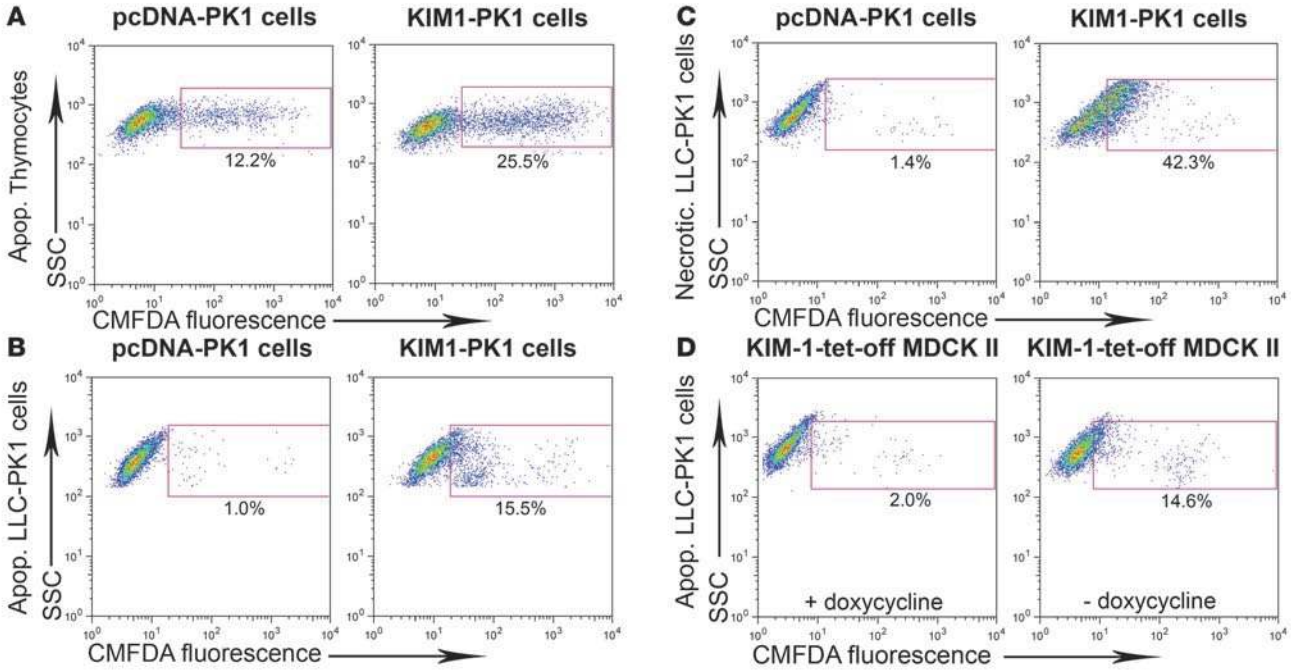

Figure 4

Quantitative analysis of KIM-1–mediated apoptotic cell and necrotic material phagocytosis. Flow cytometric plots of green fluorescence against side scatter (SSC) for KIM1-PK1 and pcDNA-PK1 epithelial cells that have ingested fluorescently labeled (CMFDA) apoptotic thymocytes (**A**), apoptotic LLC-PK1 cells (**B**), or necrotic debris (necrotic LLC-PK1 cells) (**C**) in a phagocytosis assay. Percentages represent the proportion of epithelial cells that have ingested fluorescently labeled material. KIM1-PK1 cells that have not ingested apoptotic cells or debris were used to define the gated area. Without coculture with necrotic cells, only 0.93% of KIM-1–expressing epithelial cells were identified in the gated area. (**D**) Flow cytometric plots of green fluorescence against side scatter for KIM1–tet-off MDCK epithelial cells that have ingested fluorescently labeled (CMFDA) apoptotic LLC-PK1 in a phagocytosis assay. MDCK cells were either treated with doxycycline (100 ng/ml) to inhibit expression of the KIM-1 (left panel) or no doxycycline was used (5 days), permitting high-level expression of KIM-1 (right panel). Values represent the percentage of epithelial cells that have ingested fluorescently labeled apoptotic cells. KIM1–tet-off MDCK cells that have not ingested apoptotic cells or debris were used to define no ingestion.

epithelial cells was dependent on the conditional expression of KIM-1 in the MDCK cells (induced, 11.60% ± 2.75% of cells ingested apoptotic cells vs. not induced, 2.04% ± 0.23%; Figure 4D). Phagocytosis but not binding of apoptotic cells by KIM1-PK1 cells was inhibited by pretreatment with cytochalasin D and nocodazole, inhibitors of actin filament polymerization and microtubule formation, respectively (Figure 5B). These findings in stably transfected kidney epithelial cell lines supported the role we had identified for KIM-1 in vivo (Figure 1) and in primary epithelial cell cultures (Figure 2).

KIM1-PK1 cells did not bind or internalize fluorescently labeled zymosan–Texas Red (0.5 mg/ml), latex beads–FITC (1:800 dilution), or heparin-FITC (25 μg/ml) when compared to pcDNA-PK1 cells (Figure 5C). This likely reflects lack of expression of receptors such as scavenger receptor A (SRA) as well as other components of the myeloid phagocytic machinery by the epithelial cell.

To determine whether KIM-1 expression also conferred enhanced capacity to ingest necrotic cellular debris, we prepared necrotic fluorescently labeled LLC-PK1 cells by sonication. Fifteen times more KIM1-PK1 cells ingested necrotic cell debris (32.9% ± 8.4%) as compared with control pcDNA-PK1 epithelial cells (1.9% ± 1.0%) as assessed by flow cytometry and confirmed by microscopy (Figure 3C and Figure 4C). Thus, KIM1-PK1 cells internalize apoptotic and necrotic cells.

Matrix proteoglycans such as heparan sulfate have been reported to act as opsonins for the clearance of apoptotic cells and necrotic debris (18), but in these studies, heparin, a heparan sulfate, did not bind to KIM1-PK1 cells. To determine the role of other opsonins, such as complement proteins and thrombospondin, we prepared apoptotic cells in serum free media and performed phagocytosis assays in the absence of serum. There was no difference in phagocytosis of apoptotic thymocytes by KIM1-PK1 cells in the presence (20.9% ± 1.6% KIM1-PK1 cells phagocytosed apoptotic cells) or absence (28.6% ± 5.2%) of serum, suggesting that serum-derived opsonins play no role in KIM-1 mediated phagocytosis. To show further specificity of KIM-1 in phagocytosis, we expressed the archetypal scavenger receptor SRA in LLC-PK1 cells. Although SRA promoted avid binding of apoptotic thymocytes, there was only a small increase in phagocytosis, 5.1 ± 0.3% versus 4.2 ± 0.3% (control), confirming the uniqueness of KIM-1 as a phagocytic receptor.

Our studies of rat primary epithelial cells indicated that rat Kim-1 was functioning directly as a phagocytic receptor (Figure 2). We next evaluated whether the enhanced phagocytosis conferred by human KIM-1 expression in KIM1-PK1 cells was directly due to KIM-1 functioning as an apoptotic receptor or indirectly due to upregulation of the intrinsic phagocytic machinery. Pretreatment of apoptotic cells with soluble KIM-1 ectodomain-Fc fusion protein (KIM1-Fc) (0.8 μg/ml) inhibited uptake into KIM1-PK1 cells (Figure 5D). Likewise, pretreatment of KIM1-PK1 cells with an anti–Kim-1 antibody that binds to the Ig domain (AWE2) also inhibited phagocytosis of apoptotic cells (Figure 5D), which together with the rat primary studies indicates KIM-1 binds to apoptotic cells via the Ig-domain. To further enhance the certainty that the KIM-1

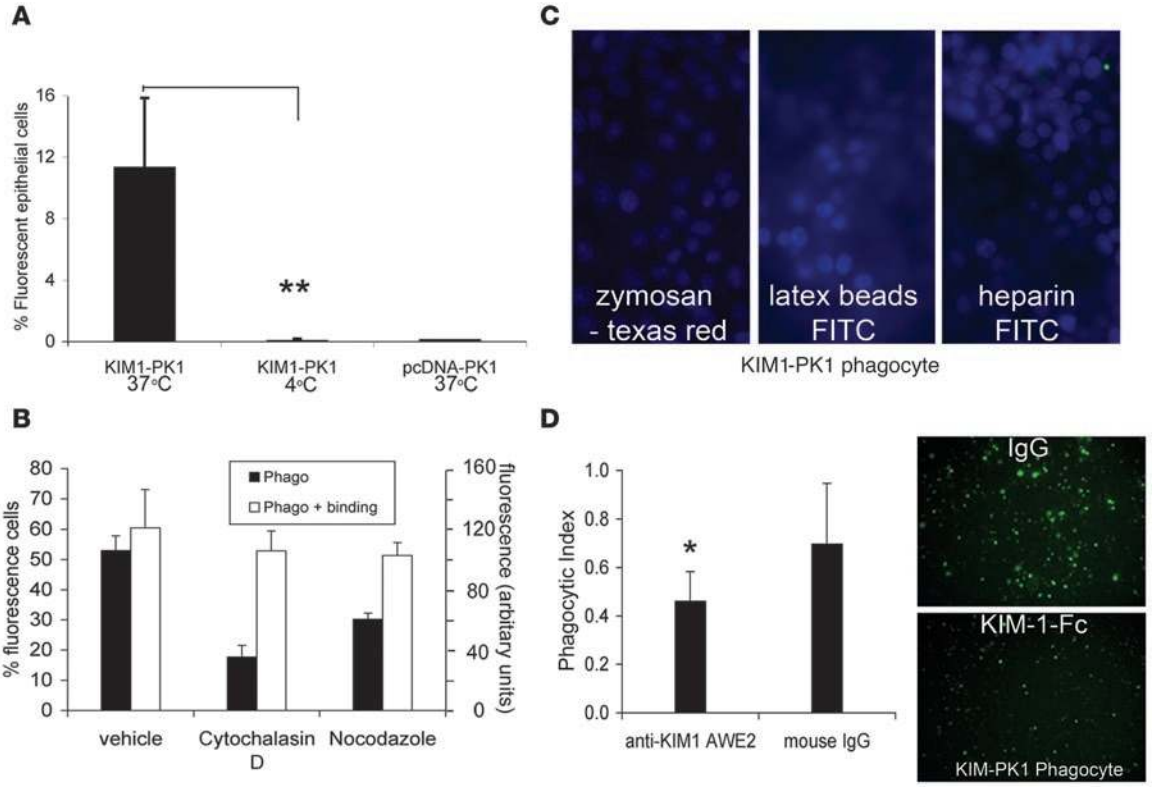

Figure 5

KIM-1 mediates phagocytosis of apoptotic necrotic cells but not other phagocytotic targets, zymosan or latex beads. (**A**) Graph showing percentage of KIM1-PK1 or pcDNA-PK1 cells that have internalized fluorescent apoptotic LLC-PK1 cells after 1 hour incubation with apoptotic fluorescent green labeled cells at 37°C or 4°C (on ice). At 4°C, binding but not internalization occurs. KIM1-PK1 cells showed much less fluorescence at 4°C than at 37°C (**$P = 0.006$; $n = 3$ per condition; error bars indicate SD). (**B**) Graph showing phagocytosis (black bars) by KIM1-PK1 cells as assessed by flow cytometry (left axis; percentage fluorescent cells) or binding plus phagocytosis (white bars) as assessed by spectrophotometry (right axis; relative fluorescence intensity). Labeled apoptotic thymocytes were incubated with KIM1-PK1 cells that had been pretreated with cytochalasin D (30 μM), nocodazole (30 μM), or vehicle. Total (bound plus phagocytosed) thymocytes were equivalent in each group; however, phagocytosis was inhibited by cytochalasin D and nocodazole. (**C**) Fluorescence images of KIM1-PK1 cells following coincubation with fluorescence-labeled zymosan particles (left, 0.5 mg/ml), latex beads (center, Fluorosphere; 1:800 dilution), or heparin (right, 25 μg/ml) for 1 hour at 37°C. Note no uptake of any of these particles. (**D**) Preincubation of KIM1-PK1 cells with anti–Kim-1 antibodies (AWE2), but not IgG, reduced phagocytic index (number of apoptotic LLC-PK1 cells/KIM1-PK1 phagocyte) as assessed by flow cytometry (50 μg/ml, left panel). Right panels show photomicrographs of KIM1-PK1 cells after internalization and binding of CMFDA-labeled apoptotic LLC-PK1 cells that had been pretreated (1 hour) with soluble mKIM1-Fc (bottom right panel, 0.8 μg/ml) or IgG-treated (top right panel). Pretreatment with mKIM1-Fc inhibited phagocytosis. Original magnification, ×40 (**C**); ×10 (**D**).

ectodomain in cells was directly responsible for binding and internalization by acting as a phagocytic receptor, we generated a truncation mutant of KIM-1 (ΔKIM1-ecto), which expressed only 5 amino acids extracellularly but expressed the transmembrane and intracellular domain normally in cells. Compared with pcDNA-PK1 cells, the ΔKIM1-ecto–PK1 cells showed no enhancement of phagocytosis in our phagocytosis assays (data not shown).

To further underscore that the phagocytic effect of KIM-1 was a direct interaction and not due to the induction of other phagocytic receptors, we assessed KIM1-PK1 and control cells for expression of CD36 (protein) and *lox-1* (transcript) but found no expression of these phagocytic receptors. Interestingly, scavenger receptor B1 (protein) was expressed by both control and KIM1-PK1 cells at equal levels (data not shown).

The KIM-1 ectodomain binds specifically to the surface of apoptotic kidney epithelial cells and PS. To investigate the biology of KIM-1 further, we assessed binding of KIM1-Fc to cells (Figure 6). KIM1-Fc bound specifically to the surface of apoptotic cells but not the surface of normal cells (Figure 6, A and B). Control c-Ret–Fc and human IgG proteins did not adhere to apoptotic or normal cells (Figure 6, A and B). KIM1-Fc binding was abolished by addition of the calcium and magnesium chelators, EGTA and EDTA, and restored in the presence of excess calcium, indicating that binding is dependent on divalent cations (Figure 6C). Divalent cation dependence has been reported for binding of other receptors of the myeloid lineage scavenger receptor family that bind apoptotic and necrotic cells (17, 19, 20).

Unlike live cells, apoptotic cells expose membrane aminophospholipids PS and phosphatidylethanolamine (PE) on the outer leaflet of the plasma membrane (15). The exposed lipids are targets that professional phagocytes use in recognition of apoptotic cells (15). In a cell-free binding assay, we tested whether KIM-1 recognized PS, PE, phosphatidylcholine (PC), or anionic phosphatidic acid (PA) adherent to plastic wells. KIM-1 ectodomain bound specifically to PS and to a lesser extent PE but not other membrane phospholipids, PC, or PA (Figure 6E). The K_d for KIM1-Fc–binding to PS was calculated from the binding curve to be 6.3 nM. To validate this

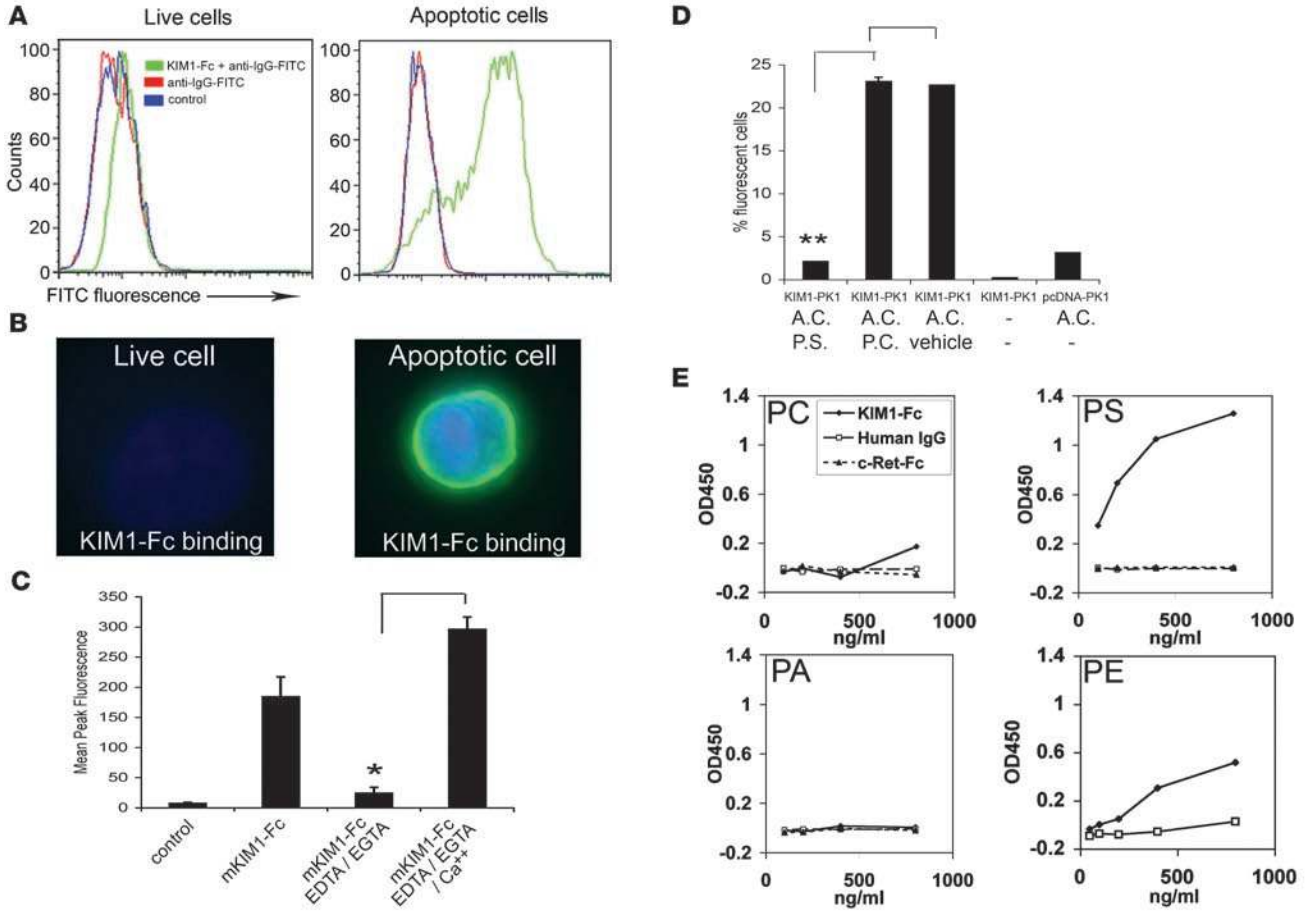

Figure 6

The KIM-1 ectodomain binds specifically to the surface of apoptotic epithelial cells and binds specifically to PS and PE. (**A**) Flow cytometric histogram plots of fluorescence of normal live LLC-PK1 epithelial cells (left panel) or apoptotic LLC-PK1 epithelial cells (right panel), labeled with KIM1-Fc followed by anti–hIgG-FITC (green), anti–hIgG-FITC alone (red), or no reagents (blue). Note an approximately 50-fold increase in binding of KIM1-Fc to apoptotic cells. (**B**) Representative photomicrographs of an apoptotic LLC-PK1 cell labeled with KIM1-Fc (green, right panel) and a normal, live LLC-PK1 cell labeled identically (left panel). Nuclei were faintly stained with DAPI (blue) in both cells. Original magnification, ×60. (**C**) Graph of mean peak fluorescence for binding of KIM1-Fc to apoptotic cells in the absence or presence of the calcium chelators EDTA/EGTA, assessed by flow cytometry. KIM1-Fc binding was abolished by calcium chelators, and binding was restored by the addition of an excess of calcium to the chelators (*P = 0.006). (**D**) Graph of phagocytosis inhibition by PS liposomes. Pretreatment of KIM-1–expressing cells with PS liposomes almost completely abolished KIM-1–mediated phagocytosis of apoptotic cells (A.C.) (**P = 0.007), while equimolar PC liposomes had no effect. Error bars indicate SD. (**E**) In vitro binding curves for purified KIM1-Fc binding to equimolar phospholipid coated ELISA plates. KIM1-Fc binding was detected by anti-human IgG — HRP conjugated antibody followed by a colorimetric assay. Note KIM1-Fc binds to aminophospholipids PS and PE but not PC or anionic phosphatidic acid (PA), whereas control Fc proteins, human IgG and c-Ret–Fc do not bind.

assay and these observations, we confirmed that PS, PE, and PC bound equally to plastic plate wells by elution of adsorbed lipids in ethanol and analysis of eluates by TLC (data not shown). These studies suggest KIM-1 is a PS receptor but may also be a receptor for PE, albeit with a lower affinity. To confirm these properties in cells, we used liposomes containing PS to competitively block uptake of apoptotic cells by KIM1-PK1 cells (15). Pretreatment of KIM1-PK1 cells with PS liposomes (0.2 mM) almost completely abolished KIM-1 mediated phagocytosis, while PC liposomes (0.2 mM) had no effect (Figure 6D). Thus, we believe KIM-1 is a novel PS receptor. In the kidney, we did not identify any interstitial cells that expressed Kim-1 (Figure 1). In particular neither resident, inflammatory macrophages, nor neutrophils expressed Kim-1. Cultured bone marrow macrophages also did not express Kim-1 by transcript or protein assessment. Furthermore, activation by LPS or dexamethasone did not induce expression of Kim-1 in macrophages that express Emr-1 (F4/80 antigen) (Figure 7). Therefore, KIM-1 appears to be unlike other epithelial apoptotic cell uptake receptors, which are similar or identical to those used by macrophages (4).

KIM-1–expressing epithelial cells bind and internalize oxidized LDL through specific interactions with the KIM-1 ectodomain. Scavenger receptors, originally named by Brown and Goldstein for their capacity to bind oxidized lipids and play a role in foam cell formation (21), participate as pattern recognition molecules in host defense and innate immunity. They have also been implicated in the tethering and internalization of apoptotic and necrotic cells (20, 22–26). The plasma membrane of healthy cells is continually oxidized, but oxidized lipids are actively transported to the inner leaflet of the membrane (27). Only in dying or necrotic cells does the outer leaflet plasma membrane retain oxidized phospholipids (28).

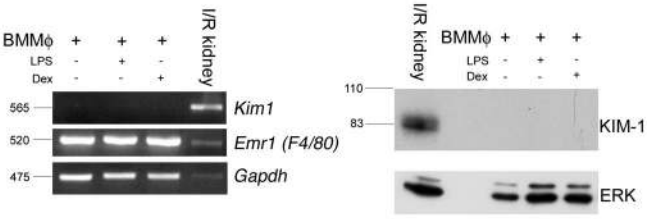

Figure 7

Macrophages do not express Kim-1/Tim-1. RT-PCR (left panel) for *Kim1* mRNA from day 7 mouse bone marrow macrophages cultured with LPS or dexamethasone. *Emr1* (F4/80 antigen) and *Gapdh* were used as controls, and mouse kidney cDNA 48 hours following ischemia was used as a positive control. Immunoblot (right panel) for Kim-1 in protein lysates from cultured macrophages and postischemic mouse kidney. Note that mouse bone marrow–derived macrophages generate neither *kim1* transcript nor Kim-1 protein, in quiescent or activated states. BMMϕ, bone marrow–derived macrophages.

Fluorescently labeled (DiI) oxidized LDL (ox-LDL) bound to KIM-1–expressing cells and was internalized at 37°C (Figure 8, A and B). Both binding to and internalization of DiI-labeled ox-LDL by KIM1-PK1 cells was totally prevented by coincubation with a 40-fold excess of unlabeled ox-LDL (Figure 8C). KIM1-PK1 cells also bound and internalized native LDL, whereas control pcDNA-PK1 cells did not (Figure 8A). Internalized ox-LDL and native LDL were both predominantly localized in intracellular vesicles (Figure 8B). Using the tet-off conditional KIM-1 expression system (Figure 8D), we confirmed that binding and internalization of ox-LDL was dependent on expression of KIM-1 (Figure 8D). It is noteworthy that while scavenger receptors class A, C, and D do not bind native LDL, scavenger receptors class B have been reported to bind native LDL as well as PS efficiently. Thus, KIM-1 shares some functional similarity with this latter class of receptors (20, 29–32).

To demonstrate that internalization of ox-LDL was mediated through direct interaction with KIM-1 ectodomain, plastic wells, coated with ox-LDL or left uncoated, were incubated with purified KIM1-Fc fusion protein or control Fc-proteins (human IgG, c-Ret–Fc). After washing away unbound Fc proteins, specific binding of KIM1-Fc was identified by colorimetric assay using horseradish peroxidase–conjugated secondary antibodies against human Fc (IgG) (Figure 8E). KIM1-Fc, but not control c-Ret–Fc or human IgG proteins, bound to ox-LDL with a K_d of 9.4 nM. We believe the ability to specifically bind to ox-LDL in addition to PS confirms KIM-1 to be a novel scavenger receptor. Since KIM-1 is not only a PS and PE receptor but also a scavenger receptor, we evaluated whether engulfment of apoptotic cells was prevented by pretreatment of KIM1-PK1 cells with ox-LDL (Figure 8F). Phagocytosis was suppressed by 76.4% (12.3% ± 1.7% vs. 2.9% ± 1.4% with 40 μg/ml ox-LDL). Some scavenger receptors bind microbial cell surface epitopes. Although KIM1-PK1 cells did not bind yeast cell wall, zymosan (Figure 5C), KIM1-PK1 cells bound and internalized both Gram negative (*E. coli*) and positive (*S. aureus*) bacteria (Figure 9).

Discussion

To date, scavenger receptors have been associated with cells of the myeloid lineage, including macrophages, dendritic cells, and, to a lesser extent, neutrophils. This is the first demonstration to our knowledge of an epithelial cell scavenger receptor involved in phagocytosis that is not expressed by myeloid lineage cells. While it shares homology with MadCam-1, an endothelial integrin and selectin receptor (33), KIM-1/TIM-1 is unique among classes of previously described scavenger receptors, all of which lack Ig super family domains (34). An epithelial scavenger receptor reportedly not expressed in myeloid cells (SCARA5) has been described, but it does not bind ox-LDL nor does it play any clear role in phagocytosis of apoptotic cells (35).

We propose that KIM-1 mediates engulfment of apoptotic and necrotic debris in the lumen of injured epithelial tubules through binding to PS and oxidized phospholipids on the surface of target cells. KIM-1 mediates phagocytosis not only by binding to the cell surface but also by triggering internalization. Our data support an important role for nonprofessional phagocytes in tissue remodeling, an area recognized to be important in invertebrates but little explored in vertebrates (36, 37). It is currently unclear whether KIM-1 triggers internalization by cooperating with a coreceptor or by signaling through its cytoplasmic tail, which contains 3 potential tyrosine phosphorylation sites (38). KIM-1 converts epithelial cells into highly phagocytic cells that exhibit phagocytic characteristics similar to those shown by professional phagocytes (15, 17). By so doing, KIM-1 may play an important role in limiting the autoimmune response to injury.

KIM-1 has high binding affinity to PS and somewhat lower affinity for PE. Another scavenger receptor, LOX-1 has been reported to bind PS but not bind PE, and we did not find evidence of its expression in kidney epithelial cells (20, 39). We did find evidence of low-level scavenger receptor B1 expression in our cell lines, which was unaffected by KIM-1 expression and does not play any role in the KIM-1 mediated phagocytosis or lipid uptake we report here. Both PS and PE are externally translocated to the outer leaflet of plasma membrane during apoptosis (40, 41). A bridging molecule for αVβ5 integrin–mediated apoptotic cell phagocytosis is milk fat globular–EGF-factor 8 (MFG-E8), which binds both PS and PE (42). Thus, KIM-1's affinity to bind aminophospholipids directly might be crucial to efficient binding and engulfment of apoptotic and necrotic cells without the need for bridging molecules.

Several PS-binding proteins and their domain structures are known; however, it is not clear whether these are conserved PS-binding domain motifs (20, 39, 42). Ig domains are components of antibodies, receptors, and adhesion molecules, and they function in recognition and binding of molecular structures. The crystal structure of mouse Kim-1 was elucidated (43), and its Ig domain has 2 binding sites for a homophilic interaction and a potential ligand binding site. A prototypical PS-binding domain, called the calcium-binding domain 2 (C2 domain), shares an antiparallel β-sheet "sandwich-like" structure (44) with the Ig domain of KIM-1. Thus, although speculative, the KIM-1–Ig domain may bind to aminophospholipids at the β-sheet–like structure, with calcium as a cofactor. Our antibody blocking data suggest that the KIM-1–Ig domain is responsible for binding to PS. In studies using KIM-1 truncation mutants, we have confirmed that the extracellular domain is responsible for all the enhanced binding capacity conferred by KIM-1 expression to apoptotic cells (data not shown). Further studies using mutated KIM-1 constructs will be required to determine the precise region responsible for PS binding and to determine whether ox-LDL–binding sites and PS-binding sites are identical or located at different sites of the protein. The in vitro binding studies indicate that KIM-1 has a higher affinity for PS than for ox-LDL. However, these studies do not necessarily indicate the relative affinity of KIM-1 for PS or

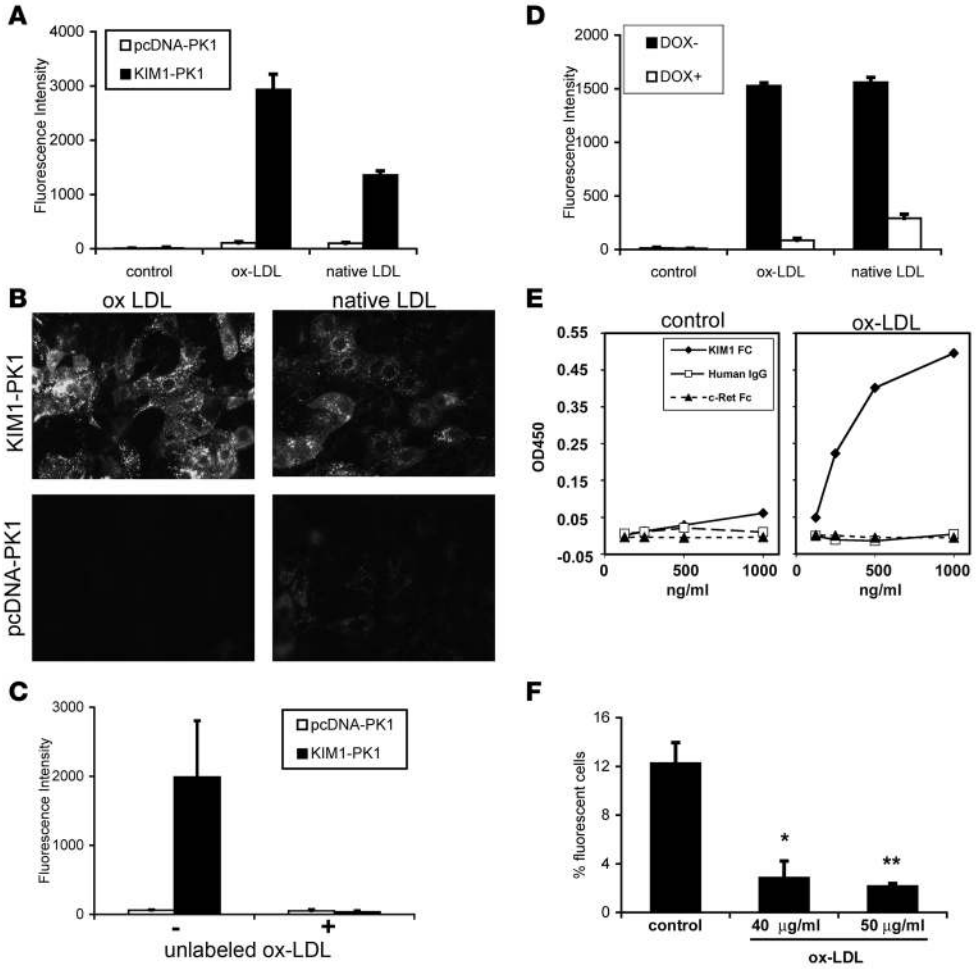

Figure 8

KIM-1–expressing epithelial cells bind and internalize ox-LDL, and the KIM-1 ectodomain binds specifically to ox-LDL. (**A**) Graph showing internalization of DiI-labeled ox-LDL or native LDL by KIM1-PK1 cells or pcDNA-PK1 cells over 1 hour at 37°C, as quantified by spectrofluorometry of lysed cells. (**B**) Photomicrographs of KIM1-PK1 cells and pcDNA-PK1 cells showing internalized ox-LDL or native LDL in intracellular vesicles. Original magnification, ×40. (**C**) Graph showing the effect of a 40-fold excess of unlabeled ox-LDL on internalization of DiI-labeled ox-LDL by KIM1-PK1 cells or pcDNA-PK1 cells incubated at 37°C for 1 hour. Uptake of fluorescent lipoprotein was quantified by spectrofluorometry of lysed cells. (**D**) Graph showing the effect of doxycycline on KIM1–tet-off MDCK cells' capacity to internalize DiI-labeled ox-LDL and DiI-labeled native LDL. In the presence of doxycycline (DOX+), KIM-1 expression is suppressed. In these conditions, there is little uptake of labeled lipoprotein after 1 hour. In the absence of doxycycline (DOX-), KIM-1 expression is not suppressed, and there is marked uptake of both lipoproteins. (**E**) In vitro binding curves for purified KIM1-Fc, human IgG1, or c-Ret–Fc proteins to ox-LDL coated ELISA plates. KIM1-Fc binding was detected by anti-human IgG – HRP-conjugated antibody followed by a colorimetric assay. Note KIM1-Fc strongly binds to ox-LDL but not uncoated plastic, whereas control proteins human IgG and c-Ret–Fc do not bind ox-LDL or plastic. (**F**) Graph showing the effect of pretreatment of KIM1-PK1 cells with either 40 or 50 μg/ml of ox-LDL on phagocytosis of fluorescently labeled apoptotic LLC-PK1 cells as assessed by flow cytometry. (*P = 0.0009 [40 μg/ml ox-LDL]; **P = 0.0003 [50 μg/ml ox-LDL] compared with no ox-LDL pretreatment. Error bars indicate SD).

oxidized phospholipids that are present on the apoptotic cell surface. Further studies will be required to determine whether different apoptotic cell types or different stages of transition from early apoptosis through late apoptosis to necrosis selectively expose oxidized phospholipids or PS to the KIM-1 receptor.

Functionally, the ability of KIM-1 to phagocytose apoptotic and necrotic cells in the tubule of the kidney may be critical for remodeling after injury. For recovery of function after acute injury, it is important that the lumen of the epithelial tubule be cleared of dead cell debris in order to relieve intratubular obstruction. Furthermore, with the massive amount of injury that frequently occurs, it is vitally important that an immune response to newly revealed tissue antigens be minimized (1). Macrophages are normally assigned to the task of clearing necrotic and apoptotic debris. However, within the epithelial tubule, macrophages are rarely if ever seen. We propose that epithelial tubule injury in other organs will require surviving epithelial cells to use phagocytic receptors such as KIM-1 and function as phagocytes for successful repair and resolution of injury. Mice lacking the phagocytic bridging molecule MFG-E8 exhibit a range of defects, resulting in autoimmunity due to aberrant phagocytosis of apoptotic and necrotic cells by dendritic cells. The mice, however, also exhibit a mammary gland phenotype due to impaired phagocytosis of dying cells by surviving epithelial cells during mammary gland involution. Epithelial cells, functioning

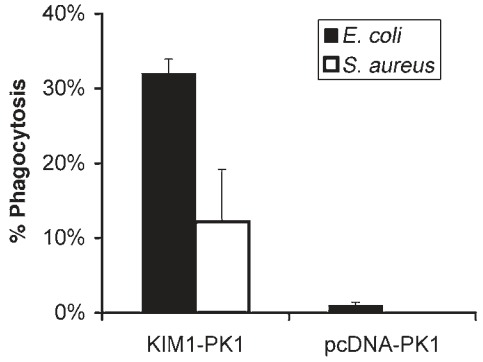

Figure 9
KIM1-PK1 cells but not pcDNA-PK1 cells bind and internalize gram negative (*E. coli*) and gram positive (*S. aureus*) bacteria. KIM-1 increases the capacity of epithelial cells to phagocytose both *E. coli* and *S. aureus* bacteria. % Phagocytosis, percentage of cells with internalized bacteria. Error bars indicate SD.

as semiprofessional phagocytes, have been implicated in normal involution of the mammary gland and therefore, tissue remodeling (45). It is interesting that in preliminary studies we have identified KIM-1 in highly phagocytic epithelial cells of day 3 involuting mammary gland (data not shown), suggesting that KIM-1 may play a broader role in epithelial remodeling.

Additional studies in vivo using targeted deletion of Kim-1 and possibly other members of the Kim family of receptors will be instructive once the animals are available. In rodents, there are 8 members of the *Tim/Kim* gene family, whereas in humans there are only 3 genes. It is possible that, in vivo, in mice deletion of more than 1 *Kim* gene will be required if there is a redundancy of function.

Phagocytosis of apoptotic cells mediated by KIM-1 may result in the generation of antiinflammatory cytokines as occurs with phagocytosis by macrophages (5–7), which also become resistant to activation by proinflammatory cytokines. Interestingly, hepatocyte growth factor (HGF), a well known renal repair factor (46), was reported to be upregulated in epithelial cells that phagocytosed apoptotic cells (7). In a preliminary study, we found upregulation of *HGF* mRNA by KIM-1 expression in LLC-PK1 cells (unpublished observations). Although speculative, KIM-1 may contribute to not only clearance of dead cells but also the regenerative mechanism, resulting in replacement of cells and restoration of the epithelium.

In conclusion, KIM-1, which is expressed on human and rodent epithelial cells following injury to the kidney, confers endocytic and phagocytic phenotypes on epithelial cells with resultant internalization of lipoproteins and apoptotic cells. To our knowledge, KIM-1 represents the first described epithelial PS and scavenger receptor that is not expressed on myeloid cells. The data presented in this study suggest that these capacities conferred by KIM-1 may facilitate remodeling of the injured epithelia.

Methods

Animal model. Ischemia reperfusion injury of the rat kidney was carried out as previously described (47). In brief, anesthetized SD rats were maintained at 36.5–37.5°C. Kidneys were exposed via flank incisions and subjected to bilateral renal artery clamping using microaneurysm clamps and returned to the retroperitoneum. After 30 minutes, the clamps were removed and kidneys confirmed to reperfuse. Wounds were closed. Experiments were carried out according to protocols approved by the Center for Animal Resources and Comparative Medicine, Harvard Medical School.

Materials. LLC-PK1 and COS-7 cell lines were from the ATCC, and FBS, DMEM, and DMEM/F-12 were from Cellgro. Generation of anti–Kim-1 antibodies AWE2.1, ABE3, ACA, and R9 was described previously (9, 48), and secondary antibodies were from DakoCytomation or Jackson ImmunoResearch Laboratories Inc. Labeled and unlabeled native LDL and ox-LDL were from Intracel Corp., and CMFDA was from Invitrogen. Human TNF-α was from Peprotech Inc. Other reagents were from Sigma-Aldrich.

Cell culture. Primary cultures of kidney proximal tubule cells were generated using established methods with modifications (12). Briefly, the kidney cortex was dissected from medulla, diced, and then digested in a solution of collagenase (0.5 mg/ml) (with soybean trypsin inhibitor) for 30 minutes at 37°C in a water bath rocker. The enzyme reaction was terminated with horse serum. Glomeruli and remaining tissue clumps were separated by decanting after gravity sedimentation (2 minutes). After washing 2 times in PBS, tubules were resuspended in tubule medium (DMEM/F-12 with transferrin, insulin, selenium, hydrocortisone, and EGF) and aliquoted into collagen I–coated tissue culture grade dishes containing autoclaved glass coverslips. Every second day, medium was replaced with fresh medium. The epithelial cells were used in assays between day 4 and day 5. KIM1-PK1 cells were generated by transfecting LLC-PK1 cells with human *KIM-1* full-length cDNA (48) subcloned into a pcDNA3 mammalian expression vector (Invitrogen) to generate a KIM-1 expression construct. This construct was transfected using Lipofectamine (Invitrogen), and stable transfectants selected for G418 resistance. Control (pcDNA-PK1) cells were generated using an empty pcDNA3 vector. Clones were isolated by limiting dilution, and KIM-1 protein expression was confirmed by both western blot and immunofluorescence using anti-human KIM-1 mouse monoclonal antibodies (AKG7, AWE2) or anti-human KIM-1 rabbit polyclonal antibody (#1400) as primary antibodies (48). Two pairs of KIM-1–expressing cells and control cells were used for the phagocytosis assay.

KIM1–tet-off MDCKII cells were generated by using BD Tet-Off Gene Expression System kit (Clontech) and MDCK–tet-off cells (Clontech). The human *KIM-1* cDNA was subcloned into pTRE-hygro constructs to generate pTRE–KIM-1, and the construct transfected into MDCK–tet-off cells (Clontech). Transfected and selected KIM1–tet-off MDCK cell clones were cultured in DMEM/F-12/10% FCS, 250 μg/ml hygromycin, and 100 μg/ml G418. Cells were cultured in 100 ng/ml doxycycline to prevent *KIM1* transcription until induction was induced by its withdrawal.

KIM-1–GFP cells were generated by subcloning human ORF *KIM1* (full length) into pEGFP N1 (Clontech), generating a fusion construct with EGFP at the C terminus. The construct was transfected into COS7 cells and stably expressing cells were selected (see above). ΔKIM1-ecto was generated by cloning the signaling peptide to the 5 amino acids closest to the transmembrane domain and all of the transmembrane and cytoplasmic domains into pcDNA3 vector. The ΔKIM1-ecto–PK1 cell line was generated in LLC-PK1 cells as described above. Full-length SRA-II was cloned from cDNA from mouse peritoneal macrophages into pCR2.1, then subcloned into pcDNA3. LLC-PK1 cells were transfected using Lipofectamine with pcDNA3–SRA-II or empty vector, and expression of SRA was confirmed by immunofluorescence using anti-CD204 antibodies (Serotec).

Immunolabeling. Paraffin sections were rehydrated and labeled with rabbit anti-rat Kim-1 (R9) antibody followed by biotinylated anti-rabbit secondary antibody and ABC peroxidase DAB labeling as previously described (9). PLP-fixed frozen sections were labeled with R9 antibody followed by Cy3-conjugated secondary antibody (9). Apoptotic nuclei were visualized using DAPI (Invitrogen) at 12.5 μg/ml in Vectashield (Vector Laboratories). Identification of TUNEL-positive cells in PFA-fixed tissues was described previously (49) using FITC-labeled dUTP (Roche) in a terminal deoxynucleotidyl trans-

ferase dependent reaction incubated for 1 hour at 37°C, followed by labeling with R9 antibody (9). Macrophages in kidney tissues were stained with anti-rat CD68 (Serotec) followed by Cy2-conjugated secondary antibody. KIM1-PK1 cells and pcDNA-PK1 cells were plated at 3.0×10^5 per well in a 4-well chamber slide or 1.5×10^5 per well in an 8-well chamber slide (Lab-Tek; Nunc). Washed cells were fixed with 2% PFA and permeabilized with 0.1% Triton X-100. After blocking, cells were incubated with mouse anti-human KIM-1 supernatant (clone AWE 2.1) for 1 hour, followed by anti-mouse Cy3 (1:800 dilution) for 30 minutes and then washed and mounted as described above. KIM-1–expressing tubules in the outer medulla of the kidney 48 hours postischemic injury were counted in 40× high-power fields (HPFs) ($n = 3$). The proportion containing intracellular, DAPI-stained fragmented nuclear bodies with characteristic morphological features of apoptotic bodies (50) was scored in 5 randomly selected fields. In the same HPFs, KIM-1–negative tubules were counted and scored for the proportion containing intracellular DAPI-labeled apoptotic bodies. Confocal immunofluorescence images were obtained with a NIKON TE2000 microscope with Auto DeBlur deconvolution software as previously described (49). KIM1-PK1 cells were cocultured with CMFDA-labeled apoptotic thymocytes for 2 hours, unbound cells were washed away, and the monolayer was fixed. The cellular structures were visualized by phalloidin-rhodamine staining. Rat primary cell cultures were incubated with rabbit anti-rat polyclonal antibodies (R9) and mouse anti-human cytokeratin antibodies (clone C22) as previously reported. KIM1-PK1 cells and pcDNA-PK1 cells were incubated with rabbit anti-human CD36 antibodies (gift from Simone B. Brown, University of Edinburgh Medical School, Edinburgh, United Kingdom) or goat anti-SRB1 antibodies (Abcam).

Detection of mRNA by PCR. Mouse macrophages were cultured from mouse bone marrow as previously described (51). Seven day macrophages were stimulated with LPS (500 ng/ml) or dexamethasone (500 nM) for 24 hours. RNA was purified and cDNAs were generated as previously described (52). *Kim-1*, *Emr-1*, and *Gapdh* mRNAs were detected using the following primer pairs: *Kim1*, 5′-ATGAATCAGATTCAAGTCTTC-3′, 5′-TCTGGTTTGTGAGTCCATGTG-3′; *Emr1*, 5′-TTTTCAGATCCTTGGCCATC-3′, 5′-ACACTGGGGCACTTTTGTTC-3′; *Gapdh*, 5′ ACTCCACTCGGCAAATTC-3′, 5′-CACATTGGGGGTAGGACCAC-3′. PCR was repeated 35 times using the following conditions: 94°C for 30 seconds, 50°C for 30 seconds, and 72°C for 60 seconds. Porcine *MFG-E8* and *LOX-1* transcripts were detected using primer pairs: *Mfg-e8*, 5′-ATCCCCAACAAGCAGATCAC-3′, 5′-CACTCAGAGGCACTGTTGGA-3′; *Lox-1*, 5′-CTGTGCCTGGGATTACTGGT-3′, 5′-TGTCCCTCCAGGATGTCTTC-3′. The *MFG-E8* and *LOX-1* transcripts were quantified by quantitative RT-PCR using iQ5 Real-time PCR detection system with CYBR Green Super Mix kit (Bio-Rad) as previously described (52).

Western blot analysis. Cells were lysed and lysates were prepared as previously described (53). Membranes were incubated with the mouse anti-human KIM-1 (clone ABE-3) or anti-rat Kim-1 (R9) antibodies followed by anti-mouse or anti-rabbit IgG-HRP, respectively. Bands were visualized by chemiluminescence (Western Lightning; PerkinElmer). Anti–β actin (Santa Cruz) antibodies were used for loading controls on stripped membranes (53).

Generation of KIM1-Fc fusion proteins. Soluble KIM-1 ectodomain-Fc fusion protein (KIM1-Fc) was produced by stably transfecting CHO cells with a expression construct containing KIM-1 ectodomain fused to human IgG-Fc region. KIM1-Fc was isolated from conditioned media by protein A–sepharose chromatography as described previously (48). Mouse Kim-1 ectodomain-Fc (mKim1-Fc) was produced using an adenovirus expression system. An expression construct encoding a mKim-1 ectodomain fused to human IgG1-Fc domain was generated and transfected to HEK-293 cells. Adenovirus was harvested from culture supernatants of the transfected cells, which was reapplied to transduce HEK-293 cells in large scale culture for KIM1-Fc production (53).

Preparation of apoptotic and necrotic cells. Confluent cultures of LLC-PK1 cells were treated with TNF-α (40 ng/ml) and cycloheximide (10 μM) (54). After 24 hours, nonadherent apoptotic cells were transferred and separated by centrifugation (400 *g*, 2.5 minutes), and then resuspended in DMEM. Apoptosis was confirmed by uptake of DAPI and failure to take up trypan blue (6) (49.52% ± 4.20%). Cells were labeled with CMFDA (Molecular Probes) as previously described (51). To generate necrotic cells, confluent cultures of LLC-PK1 cells were harvested and fluorescently labeled as described above. Cells were sonicated with 6 pulses using the W-375 processor (Heat Systems-Ultrasonic). Apoptotic thymocytes were prepared as previously described (6). The dispersed single cell supernatant of mouse thymocytes was exposed to dexamethasone (1 μmol/l) followed by culture for 16 hours in 10% FCS and antibiotics. Typically, more than 50% of induced cells were apoptotic (Annexin V binding; Boehringer Mannheim) and permeable to Hoescht 33342 (1 μg/ml), whereas less than 5% of those were positive for the uptake of propidium iodide (6). They were fluorescently labeled with CMFDA. Cells were collected (1,200 rpm, 2.5 minutes), resuspended in DMEM/F-12/10% FBS, and counted. In some studies, thymocytes were treated with dexamethasone in absence of serum (10% FBS) in media to identify potential serum opsonins.

Phagocytosis assays. To quantitate phagocytosis, KIM1-PK1 cells (3×10^5) or pcDNA-PK1 or ΔKIM1-ecto–PK1 cells were plated in 3.8 cm^2 wells 24 hours prior to assay. Primary proximal tubule kidney epithelial cells were grown in 3.8 cm^2 wells on glass coverslips or within the wells without passaging. CMFDA-labeled apoptotic LLC-PK1 cells (7×10^5), sonicated LLC-PK1 cells, or 2×10^6 apoptotic thymocytes were added to confluent epithelial cell layers and incubated for 1 hour at 37°C. Cells were washed vigorously 5 times with ice-cold PBS (without Mg^{++}/Ca^{++}) to remove bound and uningested apoptotic cells or debris. Primary epithelial cells, KIM1-PK1, or pcDNA-PK1 cells were harvested with 300 μl trypsin/EDTA solution and resuspended in 300 μl DMEM/10% FBS. Wells of KIM1-PK1 or pcDNA-PK1 not incubated with apoptotic cells or debris were used as a reference. Harvested cells were then subjected to flow cytometry (FACSCalibur; BD) as previously described (13, 14). Live epithelial cells were identified by the size using forward-scatter/side-scatter (FSC/SSC) ratio, and FSC/SSC characteristics of apoptotic cells or debris were excluded. Only live epithelial cell characteristics were selected for analysis of fluorescence (13, 14). Ingestion of apoptotic cells or debris was identified by a shift in green fluorescence. Data were analyzed by FlowJo 6.1.1. Mac software (Tree Star Inc.). The same methods were used for assay of phagocytosis by KIM1–tet-off MDCK cells cultured with or without doxycycline (100 ng/ml, 5 days). Aliquots of cells were taken from the flow assay and placed on slides. Ingestion of apoptotic cells or debris was confirmed visually using fluorescence and differential interference contrast images, and slides were counted by an investigator, blinded to the conditions, by microscopic counting of randomly selected fields as previously described (16) to determine the percentage of cells participating in phagocytosis or the phagocytic index. In some studies, the coincubation of epithelial cells with apoptotic cells was carried out at 4°C; in others, apoptotic cells were preincubated with human KIM1–Fc (hKIM1–Fc) (800 ng/ml, LLC-PK1 cells) or mouse KIM1-Fc (800 ng/ml, thymocytes) for 30 minutes 4°C, then washed 2 times prior to phagocytosis assay. For some primary epithelial cell experiments, mouse anti-rat Kim-1 ectodomain monoclonal antibodies (5 μg/ml of each) used in combination (C10, MARKE-2 MARKE-trap) (55) or mouse IgG were preincubated as described above, then washed away prior to the phagocytosis assay. We also conducted the phagocytosis assay for apoptotic thymocytes in the absence of serum (10% FBS) in media.

In other experiments, KIM1-PK1 cells or pcDNA-PK1 cells were preincubated with anti-human KIM-1 antibody (AWE2 50 μg/ml, 1 hour at 37°C), control mIgG, or 40 or 50 μg/ml of ox-LDL in DMEM/10%

FBS (2 hours at 37°C). After preincubation, apoptotic LLC-PK1 cells were added to the wells without replacing the ox-LDL containing media. For cytoskeleton inhibitor studies and SRA studies, KIM1-PK1 cells were preincubated with cytochalasin D (30 μM) or nocodazole (30 μM) for 1 hour prior to coincubation with CMFDA-labeled apoptotic thymocytes (1 hour), and unbound cells were washed with PBS 5 times. Surface bound plus internalized cells were quantified by fluorescence intensity per well using a fluorometer. The cells were harvested by trypsin-EDTA solution. Resuspended single cells were analyzed by flow cytometry for phagocytosis. Internalization of bacteria was assayed in 12-well plates by coincubation of KIM1-PK1 or control cells with Tetramethylrhodamine-labeled Gram positive (*S. aureus*) or Gram negative (*E. coli*) bacteria (Bio-Particles; Invitrogen) in a 1:10 (cell: bacteria) ratio for 1 hour at 37°C. After washing, internalization was manually counted by fluorescence microscopy. To evaluate internalization of other targets by KIM1-PK1 cells, the cells were cultured in 4-well chamber slide, then coincubated with Texas red–labeled zymosan particles (Figure 5C, left panel; 0.5 mg/ml; Invitrogen), FITC-labeled latex beads (Figure 5C, center panel; Fluorosphere; 1:800 dilution; Invitrogen), or FITC-conjugated heparin (Figure 5C, right panel; 25 μg/ml) for 1 hour. Internalization was manually assayed by fluorescence microscopy.

To determine the localization of KIM-1 in relation to bound and engulfed apoptotic cells, the phagocytosis assay was carried out as described above except that the cells were cultured in chamber slides (Nunc). After incubation, noningested apoptotic cells were either washed away as described above or simply gently aspirated to leave bound cells intact. The cells in the chamber slides were fixed, permeabilized, and blocked as described above, then labeled with anti-human KIM-1 (#1400) rabbit polyclonal antibody (1:1,000) followed by anti-rabbit Cy3 (1:400) (48).

Apoptotic cell surface binding assays. Viable and apoptotic LLC-PK1 cells were prepared as described above. Briefly, 3.0×10^5 cells were placed in 0.6-cm diameter wells with 300 μl conditioned medium containing mKIM1-Fc (800 ng/ml), hIgG1 in DMEM, or DMEM containing c-Ret–Fc at same concentration, incubated (1 hour, 37°C), washed 2 times, and incubated with anti-human IgG FITC antibody (Jackson ImmunoResearch Laboratories Inc.) (1:100) for 1 hour. After final washing, cells were fixed in PFA, resuspended in FACS buffer, and assessed by flow cytometry. In some experiments, apoptotic LLC-PK1 cells were incubated with KIM1-Fc in the presence or absence of 5 mM EDTA and 1 mM EGTA. Free calcium was restored to the solution by addition of 15 mM Ca^{2+} to the binding condition with EDTA/EGTA before applying secondary antibodies.

LDL binding assay. KIM1-PK1 or pcDNA-PK1 cells were plated at 1.5×10^5 cells per 8-well chamber slide or at 3.0×10^5 in a 3.8 cm^2 well as described above. Human DiI-labeled ox-LDL (25 μg/ml; Intracell) or human DiI-labeled native LDL (25 μg/ml, Intracell) in DMEM/10% FBS was added to the cells 24 hours after plating and incubated 1 hour at 37°C (internalization) or 4°C (binding), followed by washing with ice-cold PBS 3 times, followed by fixation (2% PFA) and mounting (Vectashield/DAPI). In some experiments, after washing, cells were lysed in 0.1% TX-100 PBS, transferred to 96-well plates, and analyzed for DiI-fluorescence using a scanning fluorometer (Flexstation; Molecular Probes) (27). Specificity of binding 5 μg/ml of DiI-labeled ox-LDL was determined by competition with 200 μg/ml (40 × excess) of unlabeled human ox-LDL (Intracell).

In vitro KIM1-Fc binding assays. All phospholipids were obtained from Avanti and stored under nitrogen to prevent oxidation. The 0.6-cm wells of ELISA plates (Corning EIA/RIA plate) were coated by addition of 50 μg/well of ox-LDL or 60 nM of PS (porcine brain, 840032C), PC (chicken egg, 840051C), PE (chicken egg, 841118C), or PA (chicken egg, 84010C) in ethanol, and the solvent was dried (39). Solvent alone was used as control. After blocking with 5% BSA, hKIM1-Fc (800 ng/ml), hIgG1 (800 ng/ml), c-Ret–Fc (800 ng/ml) in PBS containing 2 mM $CaCl_2$, or buffer alone were added to different wells and incubated 37°C for 1 hour. Following washing 3 times with PBS, bound Fc proteins were quantified using anti-human IgG-HRP (Fc-HRP) antibody (Jackson ImmunoResearch Laboratories Inc.) followed by development TMB substrate and were read at OD_{405}. Adsorption and retention of phospholipids were confirmed by reextraction of lipids by ethanol from the plastic surface. Reextracted lipids were applied to silica gel TLC plates, and after development, lipid bands were visualized with iodine vapor.

Inhibition of phagocytosis by PS liposomes. PC liposomes and PS liposomes (PS/PC mixed, 1:1) were prepared immediately prior to use by sonication of phospholipids in HBSS according to manufacture's instructions (Avanti). Liposomes were mixed with 10% FBS DMEM at 0.2 mM concentration and added to KIM1-PK1 cells in 12-well plates and pretreated for 1 hour at 37°C. Labeled apoptotic thymocytes (6.66:1 ratio) were added to the liposome-pretreated KIM1-PK1 or control cells, and the flow cytometric phagocytosis assay was carried out as described above.

Statistics. Analysis of variance was used to compare data among groups. Student's *t* test was used to determine a significant difference between 2 groups. A *P* value of less than 0.05 was considered significant. All error bars indicate SD.

Acknowledgments

We thank Vishal Vaidya for purified human KIM1-Fc, Simone B. Brown for anti-CD36 antibodies, Shuei Liong Lin and Brian Nowlin for macrophage studies and SRA studies, Shan Mou for assistance with primary cell cultures and real-time PCR, and Eileen O'Leary for support. This work was supported by grants from NIDDK/NIH (DK46267 to T. Ichimura; DK073299 to J.S. Duffield; DK39773, DK72381, and DK74030 to J.V. Bonventre).

Received for publication November 13, 2007, and accepted in revised form February 29, 2008.

Address correspondence to: Takaharu Ichimura, Renal Division, Brigham and Women's Hospital, Harvard Institutes of Medicine, Room 550, 4 Blackfan Circle, Boston, Massachusetts 02115, USA. Phone: (617) 525-5961; Fax: (617) 525-5965; E-mail: tichimura@partners.org. Or to: Jeremy S. Duffield, Laboratory of Inflammation Research, Brigham and Women's Hospital, Harvard Institutes of Medicine, Room 574, 4 Blackfan Circle, Boston, Massachusetts 02115, USA. Phone: (617) 525-5914; Fax: (617) 525-5830; E-mail: jduffield@rics.bwh.harvard.edu.

The work was presented at the 40th Annual Meeting of the American Society of Nephrology in San Francisco, California, USA, on November 2–5, 2007.

1. Bonventre, J.V. 2003. Dedifferentiation and proliferation of surviving epithelial cells in acute renal failure. *J. Am. Soc Nephrol.* **14**:S55–S61.
2. Kelly, K.J., et al. 1996. Intercellular adhesion molecule-1 deficient mice are protected against renal ischemia. *J. Clin. Invest.* **97**:1056–1063.
3. Thadhani, R., Pascual, M., and Bonventre, J.V. 1996. Acute renal failure. *N. Engl. J. Med.* **334**:1448–1460.
4. Henson, P.M., and Hume, D.A. 2006. Apoptotic cell removal in development and tissue homeostasis. *Trends Immunol.* **27**:244–250.
5. Savill, J., Dransfield, I., Gregory, C., and Haslett, C. 2002. A blast from the past: clearance of apoptotic cells regulates immune responses. *Nat. Rev. Immunol.* **2**:965–975.
6. Duffield, J.S., Ware, C.F., Ryffel, B., and Savill, J. 2001. Suppression by apoptotic cells defines tumor necrosis factor-mediated induction of glomerular mesangial cell apoptosis by activated macrophages. *Am. J. Pathol.* **159**:1397–1404.
7. Golpon, H.A., et al. 2004. Life after corpse engulfment: phagocytosis of apoptotic cells leads to VEGF secretion and cell growth. *FASEB J.* **18**:1716–1718.

8. Monks, J., et al. 2005. Epithelial cells as phagocytes: apoptotic epithelial cells are engulfed by mammary alveolar epithelial cells and repress inflammatory mediator release. *Cell Death Differ.* **12**:107–114.
9. Ichimura, T., et al. 1998. Kidney injury molecule-1 (KIM-1), a putative epithelial cell adhesion molecule containing a novel immunoglobulin domain, is up-regulated in renal cells after injury. *J. Biol. Chem.* **273**:4135–4142.
10. Han, W.K., et al. 2005. Human kidney injury molecule-1 is a tissue and urinary tumor marker of renal cell carcinoma. *J. Am. Soc. Nephrol.* **16**:1126–1134.
11. Ichimura, T., Maier, J.A.-M., Maciag, T., Zhang, G., and Stevens, J.L. 1995. Fibroblast growth factor-1 (acidic FGF) in normal and regenerating kidney: expression in mononuclear, interstitial and regenerating epithelial cells. *Am. J. Physiol.* **269**:F653–F662.
12. Sheridan, A.M., et al. 1993. Renal mouse proximal tubular cells are more susceptible than MDCK cells to chemical anoxia. *Am. J. Physiol.* **265**:F342–F350.
13. Brown, S., et al. 2002. Apoptosis disables CD31-mediated cell detachment from phagocytes promoting binding and engulfment. *Nature.* **418**:200–203.
14. Jersmann, H.P., et al. 2003. Phagocytosis of apoptotic cells by human macrophages: analysis by multiparameter flow cytometry. *Cytometry A.* **51**:7–15.
15. Fadok, V.A., et al. 1992. Different populations of macrophages use either the vitronectin receptor or the phosphatidylserine receptor to recognize and remove apoptotic cells. *J. Immunol.* **149**:4029–4035.
16. Savill, J., Dransfield, I., Hogg, N., and Haslett, C. 1990. Vitronectin receptor-mediated phagocytosis of cells undergoing apoptosis. *Nature.* **343**:170–173.
17. Savill, J.S., Henson, P.M., and Haslett, C. 1989. Phagocytosis of aged human neutrophils by macrophages is mediated by a novel "charge-sensitive" recognition mechanism. *J. Clin. Invest.* **84**:1518–1527.
18. Gebska, M.A., et al. 2002. High-affinity binding sites for heparin generated on leukocytes during apoptosis arise from nuclear structures segregated during cell death. *Blood.* **99**:2221–2227.
19. Hall, S.E., Savill, J.S., Henson, P.M., and Haslett, C. 1994. Apoptotic neutrophils are phagocytosed by fibroblasts with participation of the fibroblast vitronectin receptor and involvement of a mannose/fucose-specific lectin. *J. Immunol.* **153**:3218–3227.
20. Murphy, J.E., et al. 2006. LOX-1 scavenger receptor mediates calcium-dependent recognition of phosphatidylserine and apoptotic cells. *Biochem. J.* **393**:107–115.
21. Goldstein, J.L., and Brown, M.S. 1978. Familial hypercholesterolemia: pathogenesis of a receptor disease. *Johns Hopkins Med. J.* **143**:8–16.
22. Franc, N.C., Dimarcq, J.L., Lagueux, M., Hoffmann, J., and Ezekowitz, R.A. 1996. Croquemort, a novel Drosophila hemocyte/macrophage receptor that recognizes apoptotic cells. *Immunity.* **4**:431–443.
23. Platt, N., Suzuki, H., Kurihara, Y., Kodama, T., and Gordon, S. 1996. Role for the class A macrophage scavenger receptor in the phagocytosis of apoptotic thymocytes in vitro. *Proc. Natl. Acad. Sci. U. S. A.* **93**:12456–12460.
24. Savill, J., Hogg, N., Ren, Y., and Haslett, C. 1992. Thrombospondin cooperates with CD36 and the vitronectin receptor in macrophage recognition of neutrophils undergoing apoptosis. *J. Clin. Invest.* **90**:1513–1522.
25. Shiratsuchi, A., Kawasaki, Y., Ikemoto, M., Arai, H., and Nakanishi, Y. 1999. Role of class B scavenger receptor type I in phagocytosis of apoptotic rat spermatogenic cells by Sertoli cells. *J. Biol. Chem.* **274**:5901–5908.
26. Wang, X., et al. 2003. Cell corpse engulfment mediated by C. elegans phosphatidylserine receptor through CED-5 and CED-12. *Science.* **302**:1563–1566.
27. Chang, M.K., et al. 1999. Monoclonal antibodies against oxidized low-density lipoprotein bind to apoptotic cells and inhibit their phagocytosis by elicited macrophages: evidence that oxidation-specific epitopes mediate macrophage recognition. *Proc. Natl. Acad. Sci. U. S. A.* **96**:6353–6358.
28. Balasubramanian, K., and Schroit, A.J. 2003. Aminophospholipid asymmetry: a matter of life and death. *Annu. Rev. Physiol.* **65**:701–734.
29. Greenwalt, D.E., et al. 1992. Membrane glycoprotein CD36: a review of its roles in adherence, signal transduction, and transfusion medicine. *Blood.* **80**:1105–1115.
30. Platt, N., and Gordon, S. 1998. Scavenger receptors: diverse activities and promiscuous binding of polyanionic ligands. *Chem. Biol.* **5**:R193–R203.
31. Rigotti, A., Acton, S.L., and Krieger, M. 1995. The class B scavenger receptors SR-BI and CD36 are receptors for anionic phospholipids. *J. Biol. Chem.* **270**:16221–16224.
32. Ryeom, S.W., Sparrow, J.R., and Silverstein, R.L. 1996. CD36 participates in the phagocytosis of rod outer segments by retinal pigment epithelium. *J. Cell Sci.* **109**:387–395.
33. Briskin, M.J., McEvoy, L.M., and Butcher, E.C. 1993. MAdCAM-1 has homology to immunoglobulin and mucin-like adhesionreceptors and to IgA1. *Nature.* **363**:461–464.
34. Gordon, S. 2002. Pattern recognition receptors: doubling up for the innate immune response. *Cell.* **111**:927–930.
35. Jiang, Y., Oliver, P., Davies, K.E., and Platt, N. 2006. Identification and characterization of murine SCARA5, a novel class A scavenger receptor that is expressed by populations of epithelial cells. *J. Biol. Chem.* **281**:11834–11845.
36. Liu, Q.A., and Hengartner, M.O. 1998. Candidate adaptor protein CED-6 promotes the engulfment of apoptotic cells in C. elegans. *Cell.* **93**:961–972.
37. Wood, W., et al. 2000. Mesenchymal cells engulf and clear apoptotic footplate cells in macrophageless PU.1 null mouse embryos. *Development.* **127**:5245–5252.
38. Zhang, Z., Humphreys, B.D., and Bonventre, J.V. 2007. Shedding of the urinary biomarker kidney injury molecule-1 (KIM-1) is regulated by MAP kinases and juxtamembrane region. *J. Am. Soc. Nephrol.* **18**:2704–2714.
39. Kawasaki, Y., Nakagawa, A., Nagaosa, K., Shiratsuchi, A., and Nakanishi, Y. 2002. Phosphatidylserine binding of class B scavenger receptor type I, a phagocytosis receptor of testicular sertoli cells. *J. Biol. Chem.* **277**:27559–27566.
40. Emoto, K., Toyama-Sorimachi, N., Karasuyama, H., Inoue, K., and Umeda, M. 1997. Exposure of phosphatidylethanolamine on the surface of apoptotic cells. *Exp. Cell Res.* **232**:430–434.
41. Maulik, N., Kagan, V.E., Tyurin, V.A., and Das, D.K. 1998. Redistribution of phosphatidylethanolamine and phosphatidylserine precedes reperfusion-induced apoptosis. *Am. J. Physiol.* **274**:H242–H248.
42. Hanayama, R., et al. 2002. Identification of a factor that links apoptotic cells to phagocytes. *Nature.* **417**:182–187.
43. Santiago, C., et al. 2007. Structures of T cell immunoglobulin mucin protein 4 show a metal-ion-dependent ligand binding site where phosphatidylserine binds. *Immunity.* **27**:941–951.
44. Nalefski, E.A., and Falke, J.J. 1996. The C2 domain calcium-binding motif: structural and functional diversity. *Protein Sci.* **5**:2375–2390.
45. Hanayama, R., and Nagata, S. 2005. Impaired involution of mammary glands in the absence of milk fat globule EGF factor 8. *Proc. Natl. Acad. Sci. U. S. A.* **102**:16886–16891.
46. Liu, Y., and Yang, J. 2006. Hepatocyte growth factor: new arsenal in the fights against renal fibrosis? *Kidney Int.* **70**:238–240.
47. Witzgall, R., Brown, D., Schwarz, C., and Bonventre, J.V. 1994. Localization of proliferating cell nuclear antigen, vimentin, c-fos, and clusterin in the postischemic kidney. Evidence for a heterogeneous genetic response among nephron segments, and a large pool of mitotically active and dedifferentiated cells. *J. Clin. Invest.* **93**:2175–2188.
48. Bailly, V., et al. 2002. Shedding of kidney injury molecule-1, a putative adhesion protein involved in renal regeneration. *J. Biol. Chem.* **277**:39739–39748.
49. Duffield, J.S., et al. 2005. Restoration of tubular epithelial cells during repair of the postischemic kidney occurs independently of bone marrow-derived stem cells. *J. Clin. Invest.* **115**:1743–1755.
50. Wyllie, A.H., Kerr, J.F.R., and Currie, A.R. 1980. Cell death: the significance of apoptosis. *Int. Rev. Cytol.* **68**:251–306.
51. Duffield, J.S., et al. 2000. Activated macrophages direct apoptosis and suppress mitosis of mesangial cells. *J. Immunol.* **164**:2110–2119.
52. Duffield, J.S., et al. 2005. Selective depletion of macrophages reveals distinct, opposing roles during liver injury and repair. *J. Clin. Invest.* **115**:56–65.
53. Hung, C.C., Ichimura, T., Stevens, J.L., and Bonventre, J.V. 2003. Protection of renal epithelial cells against oxidative injury by endoplasmic reticulum stress preconditioning is mediated by ERK1/2 activation. *J. Biol. Chem.* **278**:29317–29326.
54. Soler, P., Mullin, J.M., Knudsen, K.A., and Marano, C.W. 1996. Tissue remodeling during tumor necrosis factor-induced apoptosis in LLC-PK1 renal epithelial cells. *Am. J. Physiol.* **270**:F869–F879.
55. Vaidya, V.S., Ramirez, V., Ichimura, T., Bobadilla, N.A., and Bonventre, J.V. 2006. Urinary kidney injury molecule-1: a sensitive quantitative biomarker for early detection of kidney tubular injury. *Am. J. Physiol. Renal Physiol.* **290**:F517–F529.